Transp Porous Med
https://doi.org/10.1007/s11242-017-0985-y

Methane Diffusion and Adsorption in Shale Rocks: A Numerical Study Using the Dusty Gas Model in TOUGH2/EOS7C-ECBM

Weijun Shen[1,2,3,4] · **Liange Zheng**[2] · **Curtis M. Oldenburg**[2] · **Abdullah Cihan**[2] · **Jiamin Wan**[2] · **Tetsu K. Tokunaga**[2]

Received: 21 July 2016 / Accepted: 9 December 2017

Abstract Gas production from shale gas reservoirs plays a significant role in satisfying increasing energy demands. Compared with conventional sandstone and carbonate reservoirs, shale gas reservoirs are characterized by extremely low porosity, ultra-low permeability and high clay content. Slip flow, diffusion, adsorption and desorption are the primary gas transport processes in shale matrix, while Darcy flow is restricted to fractures. Understanding methane diffusion and adsorption, and gas flow and equilibrium in the low-permeability matrix of shale is crucial for shale formation evaluation and for predicting gas production. Modeling of diffusion in low-permeability shale rocks requires use of the Dusty gas model (DGM) rather than Fick's law. The DGM is incorporated in the TOUGH2 module EOS7C-ECBM, a modified version of EOS7C that simulates multicomponent gas mixture transport in porous media. Also included in EOS7C-ECBM is the extended Langmuir model for adsorption and desorption of gases. In this study, a column shale model was constructed to simulate methane diffusion and adsorption through shale rocks. The process of binary CH_4-N_2 diffusion and adsorption was analyzed. A sensitivity study was performed to investigate the effects of pressure, temperature and permeability on diffusion and adsorption in shale rocks. The results show that methane gas diffusion and adsorption in shale is a slow process of dynamic equilibrium, which can be illustrated by the slope of a curve in CH_4 mass variation. The amount of adsorption increases with the pressure increase at the low pressure, and the mass change by gas diffusion will decrease due to the decrease in the compressibility factor of the gas. With the elevated temperature, the gas molecules move faster and then the greater gas

✉ Weijun Shen
wjshen763@imech.ac.cn

1 Key Laboratory for Mechanics in Fluid Solid Coupling Systems, Institute of Mechanics, Chinese Academy of Sciences, Beijing 100190, China

2 Energy Geosciences Division, Lawrence Berkeley National Laboratory, 1 Cyclotron Road, Berkeley, CA 94720, USA

3 Institute of Porous Flow and Fluid Mechanics, Chinese Academy of Sciences, Langfang 065007, Hebei, China

4 School of Engineering Science, University of Chinese Academy of Sciences, Beijing 100049, China

Published online: 03 January 2018

diffusion rates make the process duration shorter. The gas diffusion rate decreases with the permeability decrease, and there is a limit of gas diffusion if the permeability is less than 1.0×10^{-15} m^2. The results can provide insights for a better understanding of methane diffusion and adsorption in the shale rocks so as to optimize gas production performance of shale gas reservoirs.

Keywords Shale gas reservoirs · Methane diffusion · Adsorption · Dusty gas model · TOUGH2

1 Introduction

Because of the large reserves and the advantages of lower CO_2 emissions compared to other fossil fuels, shale gas is becoming one of the most important energy sources and has attracted increasing attention (Sutton et al. 2010; Kuuskraa et al. 2011; Michiel 2011; Shen et al. 2015). Horizontal drilling and hydraulic fracturing are the main technologies to produce gas from the ultra-low-permeability shale reservoirs (Shen et al. 2016, 2017). In the recent years, due to the advances in horizontal drilling and hydraulic fracturing, gas production from shale reservoirs has drastically increased in North America (Kuuskraa et al. 2011; Wei et al. 2016; Tokunaga et al. 2017). According to a report from the U.S. Energy Information Administration, 34% of gas production in 2011 in the USA is from shale and the percent will be predicted to reach 45% by 2035.

Compared with the conventional sandstone and carbonate reservoirs, shale gas reservoirs are characterized by relatively low porosity ($\leq$ 10%), which have ultra-low permeability ($\leq$ 0.001mD) and high clay content ($\geq$ 2%) (Boyer et al. 2006; Shen et al. 2016). Besides, the pore structures in shale gas reservoirs are complex and varied, which includes organic matter, nonorganic matrix, natural fractures and pore space induced by hydraulic fractures (Shen et al. 2017). Natural gas (primarily methane) in shale gas reservoirs exists in one of three forms: (1) free gas in fractures and pores; (2) adsorbed gas on organic matter and inorganic minerals surfaces; and (3) dissolved gas in oil and water (Strapoc et al. 2010). As there exist complex pore structures and distinctive storage in shale rock, compared with conventional gas reservoirs, the gas transport in shale gas reservoirs is a complex flow process, which is strongly influenced by diffusion, adsorption and desorption (Moridis et al. 2010). And diffusion, adsorption and desorption are the primary mechanisms controlling transport in shale matrix, while the Darcy flow is dominant in fractures and the non-Darcy flow is in hydraulic fractures (Shen et al. 2016). Thus, understanding methane diffusion and adsorption, and gas flow and equilibrium in the low-permeability matrix of shale is crucial for gas shale formation evaluation and for forecasting gas production in shale gas reservoirs.

Gas diffusion is commonly described using Fick's law, a model referred to as Fickian diffusion (Oldenburg et al. 2004). A Fickian diffusion model and a parameter-estimation technique were used to estimate the gas molecular diffusion coefficient in kerogen (Etminan et al. 2014). Yuan et al. (2014) used the Fickian diffusion to study methane adsorption and diffusion in shale and thought that it played an important role in shale gas diffusion. However, the application of Fick's law to gas diffusion in porous media has been questioned by some studies (Thorstenson and Pollock 1989; Abriola et al. 1992; Oldenburg et al. 2004), and the reason was that it violated empirical relations and did not compare well with the measured data in some circumstances (Webb 1998). The Dusty gas model (DGM), which was a more complete and rigorous model to analyze gas diffusion, was preferable to Fick's law for the

low-permeability porous media (Thorstenson and Pollock 1989; Webb 2011). The DGM was incorporated in TOUGH2/EOS7C-ECBM, a modified version of EOS7C that simulated the multicomponent gas mixture transport in porous media. It is known to be more accurate in low-permeability systems using the DGM, where the pore sizes have the same scale with the mean free path of gas molecules. Besides, the extended Langmuir model (ELM) is also included in EOS7C-ECBM for adsorption and desorption of gases (Webb 2011). Although there are a few studies about methane gas diffusion in shale gas reservoirs (Wei et al. 2013), the gas flow transport in shale rocks has not been fully understood. Therefore, there is a necessity to understand methane diffusion and adsorption in shale and the effects of the problem so as to optimize gas productivity in shale gas reservoirs.

In order to understand the process of methane gas flow and equilibrium in shale gas reservoirs, in this work we constructed a column shale model to simulate methane diffusion and adsorption through shale rocks using the module EOS7C-ECBM. The gas transport processes, including the Dusty gas model for diffusion and the extended Langmuir model for gas adsorption and desorption, were considered in the model. We first analyze the process of binary CH_4-N_2 diffusion and adsorption. Then the effects such as pressure, temperature and permeability on diffusion and adsorption through shale rocks were evaluated. This work can provide insights for a better understanding of methane diffusion and adsorption behavior in shale rocks so as to optimize production strategies in shale gas reservoirs.

2 Mathematical Models and Model Description

2.1 Mathematical Models

TOUGH2 is a numerical simulation program for multidimensional fluid and heat flows of multiphase, multicomponent fluid mixtures in porous and fractured media, which is used in geothermal reservoir engineering, environmental assessment, nuclear waste disposal and zone hydrology (Pruess et al. 1999). EOS7C is an equation of state module for the TOUGH2 program for nitrogen (N_2) or carbon dioxide (CO_2) in methane (CH_4) reservoirs (Oldenburg et al. 2004). EOS7C-ECBM developed by Webb (2011), a modified version of EOS7C, includes the extended Langmuir model (ELM) for gas adsorption and desorption and the Dusty gas model (DGM) for gas diffusion, which can be used to simulate the multicomponent gas mixture transport in porous and fractured media.

According to the Langmuir relationship (Langmuir 1916), the gas storage capacity for a single gas species can be expressed as

$$G_s = G_{sL}\left[1-(w_a+w_{we})\right]\frac{P}{P+P_L} \tag{1}$$

where G_s is the gas storage capacity, sm^3/kg; G_{sL} is the dry, ash-free Langmuir storage capacity, sm^3/kg; w_a is the ash weight fraction; w_{we} is the equilibrium moisture weight fraction; P is the pressure, Pa; P_{Li} is the Langmuir pressure, Pa.

According to Eq. (1), the extended Langmuir model for gas adsorption and desorption (Law et al. 2002) for the multiple gas species may be written as

$$G_{si} = G_{sLi}\left[1-(w_a+w_{we})\right]\frac{\frac{Py_i}{P_{Li}}}{1+P\sum_{j=1}^{nc}\frac{y_j}{P_{Lj}}} \tag{2}$$

where G_{si} is the gas storage capacity of component i, sm^3/kg; G_{sLi} is the dry, ash-free Langmuir storage capacity of component i, sm^3/kg; w_a is the ash weight fraction; w_{we} is the equilibrium moisture weight fraction; P is the pressure, Pa; y_i is the mole fraction of component i in the gas phase; P_{Li} is the Langmuir pressure of component i, Pa; and nc is the number of components in the gas phase.

The general form of the Dusty Gas Model for the gas diffusion of component i (Thorstenson and Pollock 1989; Reid et al. 1987) may be written as

$$\sum_{j=1,j\neq i}^{n}\frac{y_i N_j^{\mathrm{D}} - y_j N_i^{\mathrm{D}}}{D_{ij}^{*}} - \frac{N_i^{\mathrm{D}}}{D_i^{\mathrm{K}*}} = \frac{\left(\nabla P_i - \rho_g g\right)}{\mathrm{RT}} \tag{3}$$

where the first term on the left side accounts for the molecule–molecule interactions; the second term on the left side accounts for the molecule–medium interactions; N^{D} is the molar diffusive flux; y is the gas-phase mole fraction; D_{ij}^{*} is the effective binary diffusion coefficient; $D^{\mathrm{K}*}$ is the effective Knudsen diffusion coefficient; P is the pressure; R is the gas constant; T is the temperature.

For a three-component system, the DGM equation can be written as

$$-\left[\frac{1}{D_1^{\mathrm{K}*}} + \frac{y_2}{D_{12}^{*}} + \frac{y_3}{D_{13}^{*}}\right]N_1^{\mathrm{D}} + \frac{y_1}{D_{12}^{*}}N_2^{\mathrm{D}} + \frac{y_1}{D_{13}^{*}}N_3^{\mathrm{D}} = \frac{\nabla P_1}{\mathrm{RT}} = \frac{\mathrm{P}\nabla y_1}{\mathrm{RT}} + \frac{y_1\nabla \mathrm{P}}{\mathrm{RT}} \tag{4}$$

$$\frac{y_2}{D_{21}^{*}}N_1^{\mathrm{D}} - \left[\frac{y_1}{D_{21}^{*}} + \frac{1}{D_2^{\mathrm{K}*}} + \frac{y_3}{D_{23}^{\mathrm{K}*}}\right]N_2^{\mathrm{D}} + \frac{y_{21}}{D_{23}^{*}}N_3^{\mathrm{D}} = \frac{\nabla P_2}{\mathrm{RT}} = \frac{\mathrm{P}\nabla y_2}{\mathrm{RT}} + \frac{y_2\nabla \mathrm{P}}{\mathrm{RT}} \tag{5}$$

$$\frac{y_3}{D_{31}^{*}}N_1^{\mathrm{D}} - \left[\frac{y_1}{D_{31}^{*}} + \frac{1}{D_3^{\mathrm{K}*}} + \frac{y_3}{D_{32}^{\mathrm{K}*}}\right]N_3^{\mathrm{D}} + \frac{y_3}{D_{32}^{*}}N_2^{\mathrm{D}} = \frac{\nabla P_3}{\mathrm{RT}} = \frac{\mathrm{P}\nabla y_3}{\mathrm{RT}} + \frac{y_3\nabla \mathrm{P}}{\mathrm{RT}} \tag{6}$$

where the two terms on the right side represent ordinary and Knudsen diffusion driving forces, respectively.

When the component is single, the DGM equation can be expressed as

$$N_1^{\mathrm{D}} = -D_1^{K*}\frac{\nabla P_1}{\mathrm{RT}} \tag{7}$$

where the Knudsen diffusion coefficient models the slip of the gas, or the Klinkenberg effect.

The Knudsen diffusion coefficient (D_k) can be calculated from the following equation

$$D_{jk} = D_{\mathrm{air}k}\sqrt{\frac{m_{\mathrm{air}}}{m_j}} = k\frac{0.11k^{-0.39}}{\mu_{\mathrm{air}}}\sqrt{\frac{m_{\mathrm{air}}}{m_j}} \tag{8}$$

where k is in m^2 (Heid et al. 1950; Thorstenson and Pollock 1989).

For the ordinary diffusion, the effective diffusion coefficients are the binary gas values and can be calculated from the following equation

$$D_{ij,PT} = D_{ij}(P_0, T_0)\frac{P_0}{P}\left(\frac{T + 273.15}{273.15}\right)^{\theta} \tag{9}$$

where P_0 and T_0 are 10^5 Pa and 0 °C, respectively; and $D_{ij}^{*} = D_{ij,PT}\phi\tau_0\tau_\beta$, τ_0 is the medium tortuosity; τ_β is the saturation-dependent tortuosity (Pruess et al. 1999).

2.2 Model Description

In order to understand the process of methane diffusion and adsorption in shale rocks, here we construct a column shale model. The geometry of the shale model is shown in Fig. 1, and the properties of the shale model are summarized in Table 1. Properties of the mixtures of gaseous H_2O, N_2, CH_4 are modeled using the Peng–Robinson equation of state with enhancements (Poling et al. 2001), and solubilities are calculated using the Henry's law (Cramer 1982). The connate water exists in the shale model, and the three components H_2O, N_2 and CH_4 are modeled in a fully coupled manner in the DGM. The basic shale model assumptions are as follows: (1) The column contains the three components of H_2O, N_2, CH_4, while H_2O is minor in the gas phase; (2) the outer boundaries are closed except for the top boundary which

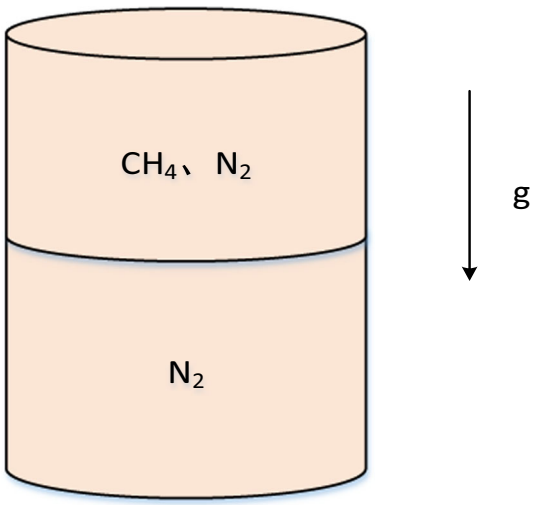

Fig. 1 Schematic of the column shale model for methane diffusion and adsorption

Table 1 Properties of the column shale model for CH_4 adsorption and diffusion

Property	Value	Unit
Model radius	4.0×10^{-2}	m
Model height	5.0×10^{-3}	m
Porosity	5	%
Permeability	1.0×10^{-15}	m^2
N_2 diffusivity	1.8×10^{-5}	m^2/s
CH_4 diffusivity	2.4×10^{-5}	m^2/s
Binary diffusivity	2.4×10^{-6}	m^2/s
Ash weight fraction	92.91	%
Equilibrium moisture weight fraction	0.8	%
Langmuir storage capacity	0.0037	sm^3/kg
Langmuir pressure	15694	Pa
Initial temperature	30	°C
Initial pressure	1.0×10^6	Pa

is open; (3) the initial condition of the model has a uniform constant temperature of 30 °C and constant pressure of 1 MPa; (4) there is nitrogen in the model system, and the top boundary is held at a constant concentration of 99% methane and 1% nitrogen, and the content of water in the gas phase is close to zero; (5) the porosity and permeability of the model are constant. The simulation was run for a base case using the module of TOUGH2/EOS7C-ECBM and in cases in which parameters such as pressure, temperature and permeability were individually varied.

3 Results and Analyses

3.1 Overview

In the beginning of the simulation, the model system is stable and there is no driving force for advection. As the simulation goes on, CH_4 will diffuse downward and N_2 in the system will diffuse upward. H_2O is a minor component in the gas phase, which plays a correspondingly minor role in the process and will not be discussed further. As CH_4 diffuses downward, the local gas density will decrease which leads to a local pressure rise below the interface. And an analogous pressure decrease will arise above the interface as N_2 diffuses into the CH_4 layer. The pressure changes give rise to potential gradients so as to cause the gas-phase advection, which is dependent on the permeability.

The gas-phase density in the N_2 and CH_4 mixtures is greatly affected by gas composition. As the pure N_2 layer is contaminated by CH_4, the local gas density decreases more than the CH_4 layer density because of N_2 contamination. As CH_4 diffuses downward, the CH_4 gas diffusing downward will be adsorbed on the shale rocks until the equilibrium state is established. Figure 2 shows the total mass of CH_4 and N_2 in the system along with gas density versus time in the model system. As illustrated in Fig. 2, the CH_4 mass increases continuously until the equilibrium while the N_2 mass decreases. The result of this imbalance

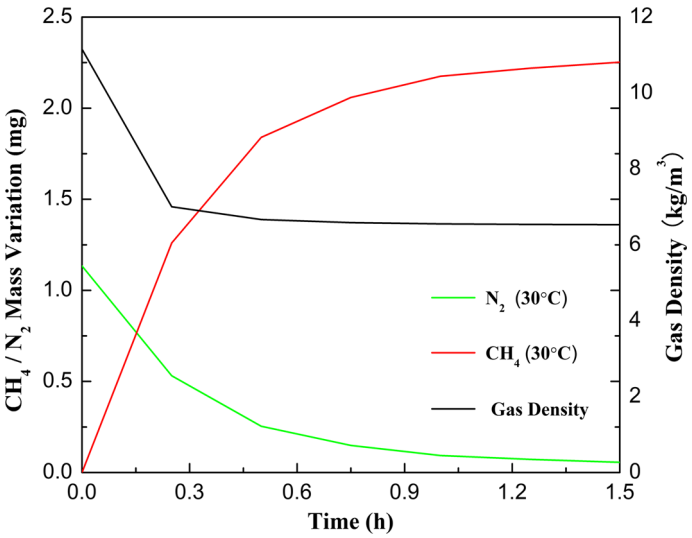

Fig. 2 CH_4/N_2 mass variation and gas density versus time

is that the pressure of the entire model system increases as the mixing progresses. In the processes of CH_4 diffusion downward and N_2 diffusion upward, the gas density in the model system will decrease continuously until the time when the CH_4 partial pressure is equal to CH_4 partial pressure at the top boundary because of the large density of N_2 relative to CH_4.

3.2 Effect of Pressure

The pressure not only affects the coverage of adsorbed gas, but also influences the adsorption heat, and then impacts the capability of the surface gas transmission (Wu et al. 2015; Wang et al. 2016). Figure 3 shows the effects of different pressures where four cases were run by varying pressure from 1 to 15 MPa to study CH_4 diffusion and adsorption. From the result of Fig. 3, with the pressure increasing in the model system, the CH_4 mass variation increases in the pressure between 1 and 5 MPa with a slight change, and the CH_4 adsorbed mass increases. In the lower pressure, the larger binding energy of gas is easy to adsorb, the pressure increases, and the amount of adsorption increases with the pressure increase (Raut et al. 2007). A longer time is required to reach an equilibrium than in a higher pressure condition. As the pressure increases further, the CH_4 adsorbed mass decreases during the process. The mass change by gas diffusion will decrease with the rising pressure due to the decrease in the compressibility factor of the gas. And the adsorbed gas amount also decreases with the rising pressure as described by adsorption isotherm (Christmann 1991; Wang et al. 2016). According to Eq. (8), it can be seen that the gas diffusion coefficient is inversely proportional to the pressure and gas diffusion is reduced by the pressure effect. With the elevated pressure, the mean free path between gas molecule collisions decreases, thereby reducing gas diffusion. In addition, we can see that there is relatively small CH_4 mass variation until the equilibrium at 1 MPa. This is because the Langmuir pressure (1.57 MPa) is larger than the pressure (1 MPa), and the shale adsorption does not attain its maximum CH_4 adsorption capacity.

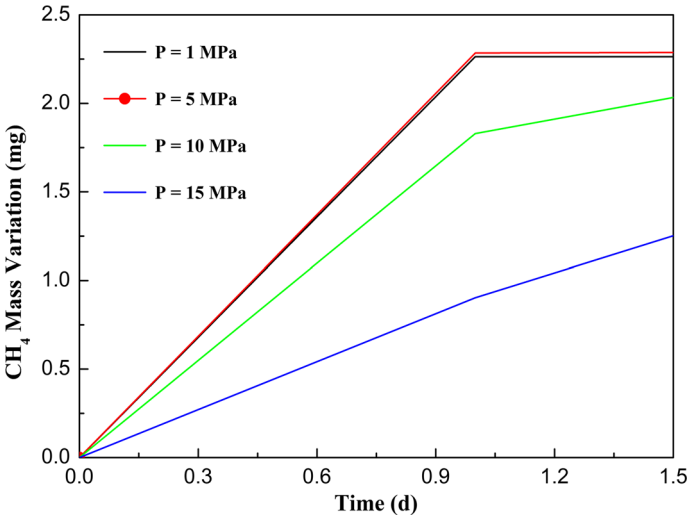

Fig. 3 CH_4 mass variation versus time for different pressure values

3.3 Effect of Temperature

Since the effect of temperature in the diffusion and adsorption process can be significant, some previous studies have focused on the effect of temperature on fractional site occupancy (Christmann 1991; Wang et al. 2016; Shen et al. 2017), which directly determines the adsorption gas amount. The desorption of adsorbed gas is an exothermic process, and the temperature influences the capacity of the surface gas transmission (Wu et al. 2015). In this study, the values of different temperatures between 30 and 150 °C are selected to investigate methane diffusion and adsorption in shale rocks. The variation of CH_4 mass variation versus time is shown in Fig. 4. As illustrated in Fig. 4, it can be seen that as temperatures increase, CH_4 mass variation increases in the process. The accumulating time for same CH_4 mass variation decreases as temperature increases at the same pressure condition. From the result of Fig. 4, the slope of a curve illustrates the rate of the diffusion–adsorption process, and the rate for 150 °C in the early stage is indicated to be somewhat greater than the corresponding rates for 30, 50 and 100 °C. However, as time elapses, the slope becomes less than that of the lower temperatures after a period of time. The incremental mass variation attained at 150 °C is also greater than that of lower temperatures in the early stage. At a higher temperature, the gas molecules move faster and have more collisions with the pore surfaces, which results in a greater adsorption rate (Wang et al. 2016; Shen et al. 2017). The greater gas diffusion rates make the process duration shorter; thus, the 150 °C curve tends to reach equilibrium sooner, which indicates that the higher temperature leads to a more quickly attained process end point.

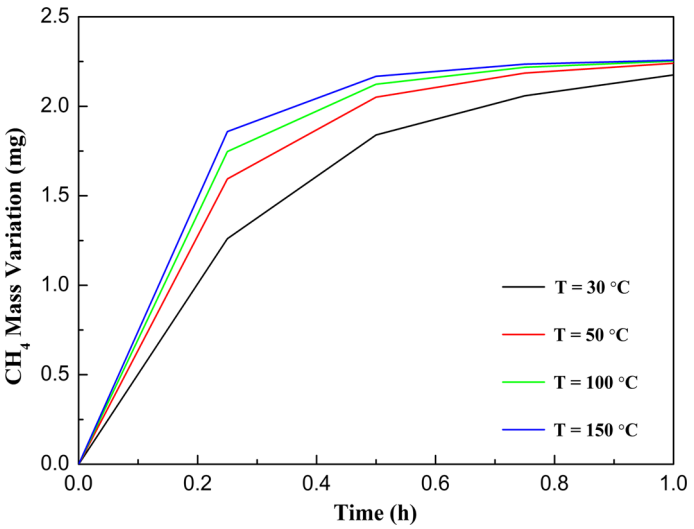

Fig. 4 CH_4 mass variation versus time for different temperature values

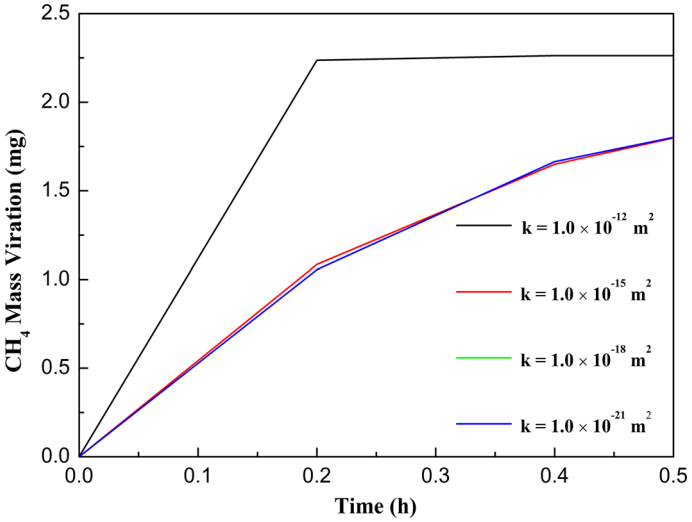

Fig. 5 CH_4 mass variation versus time for different permeability values

3.4 Effect of Permeability

Shale is a very fine-grained and clastic sedimentary rock, which is characterized by extremely low porosity, ultra-low permeability between 0.001 and 0.00001 mD (Shen et al. 2015, 2016). The permeability plays an important role in gas flow transport in shale gas reservoirs (Sun et al. 2017; Tokunaga et al. 2017). In the study, four cases of different permeability values from 1.0×10^{-12} to 1.0×10^{-21} m^2 are selected to study the effects of methane diffusion and adsorption in shale rocks, as shown in Fig. 5. From the result of Fig. 5, it can be seen that gas diffusion slows down with the permeability decrease while there is a slight change after the permeability reaches 1.0×10^{-15} m^2. The slope of a curve in Fig. 5 also explains the rate of the diffusion and adsorption process, and the rate for 1.0×10^{-12} m^2 in the early stage is illustrated to be much greater than the corresponding rates for 1.0×10^{-15}, 1.0×10^{-18} and 1.0×10^{-21} m^2. Yet with time elapsing, the slope becomes less than that of the lower permeability after a period of time. The incremental mass variation in 1.0×10^{-12} m^2 is much greater than that of lower permeability in the early stage. This suggests that the permeability has a great effect on the gas diffusion rate if the permeability is more than 1.0×10^{-15} m^2. As illustrated in Fig 5, it can be seen that there is very little change in these results between 1.0×10^{-15} and 1.0×10^{-21} m^2. It implies that there is a limit of gas diffusion when the permeability is very low at which the permeability is not the dominant factor influencing gas diffusion in shale.

4 Summary and Conclusions

In this work, a column shale model was considered to simulate methane diffusion and adsorption through shale rocks using the DGM and ELM in the module EOS7C-ECBM. The Dusty gas model was used to analyze gas diffusion, and the extended Langmuir model was included to describe gas adsorption and desorption. The change process of methane diffusion and

adsorption was analyzed, and then the effects of different pressures, temperatures and permeability values on diffusion and adsorption through shale rocks were evaluated. The result suggests that methane gas diffusion and adsorption in shale is a slow process of dynamic equilibrium, and the slope of a curve in CH_4 mass variation can illustrate the gas diffusion rate. In the lower pressure, the amount of adsorption increases with the pressure increase, and the mass change by gas diffusion will decrease with the rising pressure due to the decrease in the compressibility factor of the gas. With the elevated temperature, the gas molecules move faster and then the greater gas diffusion rates make the process duration shorter. The gas diffusion rate reduces with the permeability decrease, and there is very little change if the permeability is less than 1.0×10^{-15} m^2, and it suggests that there is a limit of gas diffusion when the permeability reaches the dividing line. This work can help to improve the understanding of gas flow transport in shale rocks and the effects of reservoir properties so as to optimize production strategies in shale gas reservoirs. In the future work, we will conduct the experiment of methane diffusion and adsorption in shale rocks and compare experimental and numerical results.

Acknowledgements This work was supported by the National Energy Technology Laboratory under U.S. Department of Energy Contract No. ESD14085, "Understanding Water Controls on Shale Gas Mobilization into Fractures," by National Science and Technology Major Project of the Ministry of Science and Technology of China Project (No. 50150503-12 and 2016ZX05037006) and by the Project of PetroChina Research Institute of Petroleum Exploration and Development (No. RIPED-LFFY-2017-JS-118). We also thank the support from the Foundation of China Scholarship Council and the Youth Foundation of Key Laboratory for Mechanics in Fluid Solid Coupling Systems, Chinese Academy of Sciences.

References

Abriola, L.M., Fen, C.S., Reeves, H.W.: Numerical simulation of unsteady organic vapor transport in porous media using the Dusty Gas Model. In: Weyer, K.U. (ed.) Subsurface Contamination by Immiscible Fluids. Balkema, Rotterdam (1992)

Boyer, C., Kieschnick, J., Suarez-Rivera, R., et al.: Production gas from its source. Oilfield Rev. **18**, 36–49 (2006)

Cramer, S.D.: The solubility of methane, carbon dioxide, and oxygen in brines from 0 to 300°C, U.S. Bureau of Mines: Report No. 8706 (1982)

Christmann, K.: Macroscopic treatment of surface phenomena: thermodynamics and kinetics of surfaces. In: Baumgärtel, H., Franck, E.U., Grünbein, W. (eds.) Topics in Physical Chemistry. Springer, Berlin (1991)

Etminan, S.R., Javadpour, F., Maini, B.B., et al.: Measurement of gas storage processes in shale and of the molecular diffusion coefficient in kerogen. Int. J. Coal Geol. **123**, 10–19 (2014)

Heid, J.G., Mcmahon, J.J., Nielsen, R.F., et al.: Study of the permeability of rocks to homogeneous fluids. Am. J. Roentgenol. **139**, 333–347 (1950)

Kuuskraa, V.A., Scott, H., Stevens, K.M.: EIA/ARI World Shale Gas and Shale Oil Resource Assessment. Advanced Resources International, Inc., Arlington (2011)

Langmuir, I.: The constitution and fundamental properties of solids and liquids. I, solids. J. Am. Chem. Soc. **184**, 102–105 (1916)

Law, D.H.S., Van Der Meer, L.G.H., Gunter, W.D.: Numerical simulator comparison study for enhanced coalbed methane recovery processes, part I: pure carbon dioxide injection. In: SPE Gas Technology Symposium, Alberta, Canada (2002)

Michiel, S., et al.: Shale Gas: A Global Perspective. KPMG Global Energy Institute, München (2011)

Moridis, G.J., Blasingame, T.A. Freeman, C.M.: Analysis of mechanisms of flow in fractured tight-gas and shale-gas reservoirs. In: SPE Latin American and Caribbean Petroleum Engineering Conference, Lima, Peru (2010)

Oldenburg, C.M., Webb, S.W., Pruess, K., Moridis, G.J.: Mixing of stably stratified gases in subsurface reservoirs: a comparison of diffusion models. Transp. Porous Med. **54**, 323–334 (2004)

Poling, B.E., Prausnitz, J.M., O'Connell, J.P.: The Properties of Gases and Liquids. McGraw Hill, New York (2001)

Pruess, K., Oldenburg, C.M., Moridis, G.J.: TOUGH2 User's Guide, Version 2. LBNL-43134. Lawrence Berkeley National Laboratory, Berkeley (1999)
Reid, R.C., Prausnitz, J.M., Poling, B.E.: The Properties of Gases and Liquids, 4th edn. McGraw-Hill Book Company, New York (1987)
Raut, U., Famá, M., Teolis, B., et al.: Characterization of porosity in vapor-deposited amorphous solid water from methane adsorption. J. Chem. Phys **127**, L357 (2007)
Strapoc, D., Mastalerz, M., Schimmelmann, A., et al.: Geochemical constrains on the origin and volume of gas in the New Albany Shale (Devonian–Mississippian), Eastern Illinois Basin. AAPG Bull. **94**, 1713–1740 (2010)
Sutton, R.P., Cox, S.A., Barree, R.D.: Shale gas plays: a performance perspective. In: SPE Tight Gas Completions Conference, San Antonio, Texas (2010)
Shen, W.J., Wan, J.M., Kim, Y., et al.: Porosity calculation, pore size distribution and mineral analysis within shale rocks: application of scanning electron microscopy. Electron. J. Geotech. Eng. **20**, 11477–11490 (2015)
Shen, W.J., Xu, Y.M., Gu, J.R., et al.: Numerical simulation of gas and water flow mechanism in hydraulically fractured shale gas reservoirs. J. Nat. Gas Sci. Eng. **35**, 726–735 (2016)
Shen, W.J., Li, X.Z., Xu, Y.M., et al.: Gas flow behavior of nanoscale pores in shale gas reservoirs. Energies **10**, 1–12 (2017)
Sun, Z., Li, X.F., Shi, J.T., et al.: Apparent permeability model for real gas transport through shale gas reservoirs considering water distribution characteristic. Int. J. Heat Mass Transf. **115**, 1008–1019 (2017)
Tokunaga, T.K., Shen, W.J., Wan, J.M., et al.: Water saturation relations and their diffusion-limited equilibration in gas shale: implications for gas flow in unconventional reservoirs. Water Resour. Res. **53**, 1–14 (2017)
Thorstenson, D.D., Pollock, D.W.: Gas transport in unsaturated zones: multi-component systems and the adequacy of Fick's Laws. Water Resour. Res. **25**, 477–507 (1989)
Yuan, W., Pan, Z., Li, X., et al.: Experimental study and modelling of methane adsorption and diffusion in shale. Fuel **117**, 509–519 (2014)
Webb, S.W.: Gas-phase diffusion in porous media: evaluation of an advective-dispersive formulation and the dusty gas model for binary mixtures. J. Porous Media **1**, 187–199 (1998)
Webb, S.W.: EOS7C-ECBM Version 1.0, Report CRC2011-0002. Lawrence Berkeley National Laboratory, Berkeley (2011)
Wei, M.Q., Duan, Y.G., Fang, Q.T., et al.: Mechanism model for shale gas transport considering diffusion, adsorption/desorption and Darcy flow. J. Cent. South Univ. **20**, 1928–1937 (2013)
Wei, M.Q., Duan, Y.G., Dong, M.Z., et al.: Blasingame decline type curves with material balance pseudo-time modified for multi-fractured horizontal wells in shale gas reservoirs. J. Nat. Gas Sci. Eng. **31**, 340–350 (2016)
Wu, K.L., Li, X.F., Chen, Z.X.: The mechanism and mathematical model for the adsorbed gas surface diffusion in nanopores of shale gas reservoirs. Sci. China Technol. Sci. **45**, 525–540 (2015)
Wang, J.J., Wang, B.E., Li, Y.J., et al.: Measurement of dynamic adsorption–diffusion process of methane in shale. Fuel **172**, 37–48 (2016)